Journal Article

Cellular Internalization of Human Calcitonin Derived Peptides in MDCK Monolayers
A Comparative Study with Tat(47-57) and Penetratin(43-58)

Author(s):
Tréhin, Rachel; Krauss, Ulrike; Muff, Roman; Meinecke, Martina; Beck-Sickinger, Annette G.; Merkle, Hans P.

Publication Date:
2004-01

Originally published in:

Pharmaceutical Research 21(1), http://doi.org/10.1023/B:PHAM.0000012149.83119.bf →

Cellular Internalization of Human Calcitonin Derived Peptides in MDCK Monolayers: A Comparative Study with Tat(47-57) and Penetratin(43-58)

Rachel Tréhin,[1] Ulrike Krauss,[2] Roman Muff,[3] Martina Meinecke,[1] Annette G. Beck-Sickinger,[2] and Hans P. Merkle[1,4]

Received August 25, 2003; accepted September 29, 2003

Purpose. The objective of this study was to evaluate key motif requirements of human calcitonin (hCT)-derived peptides for the permeation through the plasma membrane of MDCK monolayers, as epithelial model.

Methods. Truncated and sequence-modified fluorescent-labeled hCT-derived peptides were synthesized through Fmoc chemistry. Peptide uptake by confluent MDCK was observed by confocal laser scanning microscopy. The cytotoxic effect of the peptides on cellular integrity was followed by LDH release. For direct comparison we covered the cellular uptake of established cell penetrating peptides, Tat(47-57) and penetratin(43-58).

Results. Truncated sequences of hCT, from hCT(9-32) to hCT(18-32), penetrated the plasma membrane and demonstrated a sectoral, punctuated cytoplasmic distribution. The uptake process appeared to be temperature-, time- and concentration-dependent. Amino acid modifications of hCT(18-32) indicated that both the proline in position 23 and the positive charge of lysine in position 18 are crucial for peptide uptake. The reverse sequence hCT(32-18) did not penetrate the membrane, indicating the importance of sequence orientation. Tat(47-57) and penetratin(43-58) showed a similar punctuated cytoplasmic distribution in MDCK and HeLa cell lines. No relevant toxicity was observed.

Conclusions. Selected hCT-derived peptides have cell penetrating properties. The uptake mechanism seems to involve an endocytic pathway.

KEY WORDS: human calcitonin; cell penetrating peptides; cell uptake; endocytosis; MDCK.

INTRODUCTION

The therapeutic potential of peptide-, protein-, and nucleic acid-based drugs is frequently compromised by their limited ability to cross the plasma membrane resulting in poor cellular access (1,2). Conjugation of such therapeutic agents to cell penetrating peptides (CPPs) has been suggested to improve their bioavailability. Several examples of CPPs have been described so far, such as 1) HIV-1 Tat-derived peptides (3–5), 2) the third helix of the homeodomain of Antennapedia, i.e., penetratin [e.g. Antp(43-58)] (6,3) the herpes simplex virus VP22 protein (7,8,4) polyarginines (9,10). CPPs have been shown to cross cellular membranes and to deliver conjugated (or fused) biopharmaceuticals, such as peptide nucleic acids (PNAs) (11), antisense oligonucleotides (12), full-length proteins (4,13), or nanoparticles (14) and liposomes (15) into cells. The exact mechanisms underlying the translocation of CPP across the cellular membrane is still poorly understood. However, several similarities in translocation mechanism were found: the internalization of these peptides was neither significantly inhibited by low temperature, depletion of cellular ATP pool, nor inhibitors of endocytosis (3,6,10,16). Therefore, translocation was concluded to result from a direct transfer through the lipid bilayer of the cell membranes (3,6). Recently, however, the mechanisms of protein/peptide translocation have been re-evaluated and the involvement of endocytosis in cellular internalization of both CPPs and CPPs conjugated to PNAs has been suggested (17,18).

In the present study, we report on a new group of peptide sequences derived from the C-terminal domain of human calcitonin (hCT) with ability to translocate the plasma membrane of Madin–Darby canine kidney cell line (MDCK) monolayers, a meaningful cellular model for columnar-type epithelia (19,20). Our hCT-derived CPP carry a relatively low positive charge in contrast to other CPPs, which are highly positively charged (arginine- or lysine-rich) at physiologic pH (3,10,21). A previous study demonstrated that the C-terminal fragment of hCT featuring residues 9 to 32, that is, hCT(9-32), as well as human calcitonin itself are internalized *in vitro* into bovine nasal epithelium (22). Moreover, we previously showed that the green fluorescent protein conjugate GFP-hCT(9-32) was also translocated into bovine nasal epithelium (23). To further investigate the underlying principles of peptide uptake we analyzed, by confocal laser scanning microscopy (CLSM), key sequence requirements for translocation by generating a series of peptides by both truncations and sequence variations of hCT(9-32). The present work reveals that the minimally required hCT sequence that could be internalized in MDCK was hCT(18-32). For reference, the investigated hCT peptides were compared with Tat(47-57) and penetratin(43-58) using cellular uptake assays in both MDCK and HeLa cells. Once translocated into the cells all the tested peptides demonstrated a punctuated cytoplasmic distribution, suggesting the involvement of endocytosis.

MATERIALS AND METHODS

Materials

MDCK (low resistance, type II) was a gift from the Biopharmacy group, ETH (Zurich, Switzerland; Ref. 20). Cervical carcinoma cells, HeLa, were obtained from American Type Culture Collection (Rockville, MD, USA). Cell culture media, L-glutamine, penicillin, streptomycin, and phosphate-buffered saline without calcium and magnesium were from Invitrogen Corporation (Carlsbard, CA, USA). Fetal calf serum (FCS) was purchased from Winiger AG (Wohlen, Switzerland) and 5(6)-carboxyfluorescein from Fluka (Buchs, Switzerland). Hoechst 33342, LIVE/DEAD Viability/Cyto-

[1] Department of Chemistry and Applied BioSciences, Swiss Federal Institute of Technology Zurich (ETH Zurich), Winterthurerstrasse 190, 8057 Zurich, Switzerland.

[2] Institute of Biochemistry, University of Leipzig, 04103 Leipzig, Germany.

[3] Departments of Orthopaedic Surgery and Medicine, University of Zurich, Klinik Balgrist, Forchstrasse 340, 8008 Zurich, Switzerland.

[4] To whom correspondence should be addressed (e-mail: hmerkle@pharma.ethz.ch)

0724-8741/04/0100-0033/0 © 2004 Plenum Publishing Corporation

toxicity kit assay and 5(6)-carboxytetramethylrhodamin (TAMRA) were purchased from Molecular Probes (Eugene, OR, USA). Human calcitonin (hCT) was a gift from H. Rink from Novartis (Basel, Switzerland). Human calcitonin gene-related peptide (hCGRP) and human amylin (hAmylin) were purchased from Bachem (Bubendorf, Switzerland), and human adrenomedullin (hADM) from Peptide Institute in Osaka, Japan. Forskolin was from CalbioChem (San Diego, CA, USA). Tetramethyl rhodamine isothiocyanate (TRITC) dextran, lactate dehydrogenase (LDH) kits, and all other chemicals were commercially available. Cell culture inserts (polyethylene terephthalate, 4.2-cm^2 growth area, 0.4-μm pore size, 1.6×10^6 pores/cm^2) and companion plates were purchased from Falcon (Franklin Lakes, NJ, USA). Glass chamber slides were obtained from Nunc (Roskilde, Denmark). Twelve- and 24-well plates were obtained from TPP (Trasadingen, Switzerland). The used UV spectrophotometer was a Varian Cary 50. The transepithelial electrical resistance of cell monolayers grown on inserts was measured using the Millicell-ERS system from Millipore (Billerica, MA, USA).

Methods

Synthesis of hCT Fragments, Labeling, and Identification

Linear hCT fragments were synthesized according to Rist *et al.* (24) using Rink amide resin to obtain C-terminal amides. All fragments were labeled at the N-terminus with 5(6)-carboxyfluorescein or with TAMRA, whereas the peptide was still bound to the resin with fully protected side chains (25). Coupling was performed using an 8-fold excess of TAMRA or a 10-fold excess of 5(6)-carboxyfluorescein, diisopropylcarbodiimide, and 1-hydroxybenzotriazole. The overall coupling time was 30 min for 5(6)-carboxyfluorescein and 45 min for TAMRA. The 5(6)-carboxyfluorescein labeled peptides were cleaved with TFA/thioanisole/thiocresol (90:5:5, v/v/v) within 3 h at room temperature, precipitated from cold diethyl ether, and collected by centrifugation. The crude peptides were dissolved in methanol/piperidine (9:1, v/v) and shaken for 1 h to remove excess of carboxyfluorescein. For TAMRA-labeled peptide, the excess dye was removed by extensive washing with *N*,*N*-dimethylformamide, dichloromethane, ethanol and diethylether, whereas the peptide was still attached to the resin. The TAMRA-labeled peptide was then cleaved and precipitated from cold diethyl ether and collected by centrifugation. All the peptides were subsequently lyophilized.

The following sequences were synthesized (Table I). N-terminally truncated fragments: Starting from the C-terminal fragment hCT(9-32), we synthesized further peptides with various truncations, down to a total length of 9 amino acids, hCT(24-32). C-terminally truncated fragment: hCT(18-31). Amino acid replacements: Single amino acid replacements were performed in position 17, 18, 19, and 23 (see Table I for details). Extended sequences: For elongation of the C-terminal segment, we added two alanines to the C-terminus of hCT(18-32). Reverse sequence: hCT(32-18), the reverse amino acid sequence of hCT(18-32). Random sequence: A peptide sequence containing the 24 amino acids of hCT(9-32) in a random position was synthesized as a negative control.

Peptides were purified by preparative high-performance liquid chromatography (HPLC) and their purity confirmed by HPLC analysis using a LiChrospher 100 RP-18 column with a flow rate of 1 ml/min using an acetonitrile:water (containing 0.1% TFA) gradient. Fluorescence was detected at 517 nm and UV at 220 nm. The molecular weight was verified by mass spectrometry (Finnigan Mat SSQ 710/ Waters 600-MS).

Synthesis of Tat(47-57) and Penetratin(43-58), Labeling, and Identification

Synthesis of Tat(47-57) and penetratin(43-58) (see Table I) were conducted by solid phase on an Applied Biosystems 433A peptide synthesizer following the Fmoc chemistry protocol. Two glycines were added, one at the N-terminal and one at the C-terminal end of the Tat(47-57) peptide to provide links for fluorochrome binding. In the case of penetratin(43-58), the C-terminal end was amidated to improve its stability. The peptides were labeled at the N-terminus with a 3-fold excess of 5(6)-carboxyfluorescein while still bound to the resin with fully protected side chains. The overall coupling time was 3 h followed by washing steps with *N*,*N*-dimethylformamide. The peptides were cleaved with TFA/water/triisopropylsilane/ethandithiol (92.5:2.5:2.5:2.5, v/v/v/v) within 2 h at room temperature, precipitated from tert-butylmethylether, collected by centrifugation, and lyophilized.

Peptides were purified by preparative HPLC and their purity confirmed by HPLC analysis using an EC 250/4 Nucleosil 300-5 C18 with a flow rate of 1 ml/min. A linear gradient starting at 90% solvent A (water:TFA, 99.9:0.1, v/v) and 10% solvent B (acetonitrile:TFA, 99.915:0.075, v/v) to 100% solvent B over 50 min. UV detection was set at 222 nm. The molecular weights were verified by mass spectrometry (Perkin-Elmer Sciex API III Quadrupol Biomolecular Mass Analyzer).

Cell Culture

MDCK cells were grown under standard conditions in minimum essential medium with Earl's salts containing 10% heat-inactivated FCS, 1% L-glutamine and 1% penicillin/streptomycin (20). HeLa cells were cultured as exponentially growing subconfluent monolayers on 25-cm^2 culture flasks in Dulbecco's modified eagle medium (high glucose) supplemented with 10% heat-inactivated FCS and 1% penicillin/streptomycin.

CLSM

Exponentially growing MDCK and HeLa cells were seeded onto either four-well glass chamber slides or cells culture inserts, cultured 2 or 3 days for proliferating cells and 10 days for confluent cells. MDCK cells were seeded at a constant density of 2×10^4 cells/cm^2 and HeLa cells at 10^5 cells/cm^2. For confluent cells, medium was changed twice a week until confluent monolayers formed. For uptake experiments, cells were first incubated in serum free medium for 30 min. The medium was then discarded and the cells further incubated in serum-free medium containing fluorescence-labeled peptides or unconjugated fluorophore at the appropriate concentration. Simultaneously, nuclei were stained with 1 μg/ml Hoechst 33342. When appropriate, endosomes were stained with TRITC-dextran. The study was conducted at 37°C or 4°C with horizontal mechanical shaking (150 rpm). Subsequently, cells were rinsed three times with serum-free me-

Table I. Uptake of hCT-Derived Peptides, Tat(47-57) and Penetratin(43-58) in MDCK Cell Monolayers

Name	MW[a] (Da)	Sequence																											Uptake[b]
		9[c]			12			15			18			21			24			27				31			34		
hCT(9-32)	2968.5	L	G	T	Y	T	Q	D	F	N	K	F	H	T	F	P	Q	T	A	I	G	V	G	A	P			++
hCT(12-32)	2699.3				Y	T	Q	D	F	N	K	F	H	T	F	P	Q	T	A	I	G	V	G	A	P			++
hCT(15-32)	2306.3							D	F	N	K	F	H	T	F	P	Q	T	A	I	G	V	G	A	P			+
hCT(18-32)	1929.9										K	F	H	T	F	P	Q	T	A	I	G	V	G	A	P			+
hCT(19-32)	1800.5											F	H	T	F	P	Q	T	A	I	G	V	G	A	P			–
hCT(20-32)	1653.3												H	T	F	P	Q	T	A	I	G	V	G	A	P			–
hCT(21-32)	1516.2													T	F	P	Q	T	A	I	G	V	G	A	P			–
hCT(24-32)	1170.8																Q	T	A	I	G	V	G	A	P			–
hCT(18-31)	1831.6										K	F	H	T	F	P	Q	T	A	I	G	V	G	A				+
hCT(9-29)	2743.6	L	G	T	Y	T	Q	D	F	N	K	F	H	T	F	P	Q	T	A	I	G	V						–
P23A-hCT(18-32)	1902.7										K	F	H	T	F	**A**	Q	T	A	I	G	V	G	A	P			–
D-K18-hCT(18-32)	1928.7										**k**	F	H	T	F	P	Q	T	A	I	G	V	G	A	P			–
D-F19-hCT(18-32)	1928.7										K	**f**	H	T	F	P	Q	T	A	I	G	V	G	A	P			–
K18A-hCT(18-32)	1871.6										**A**	F	H	T	F	P	Q	T	A	I	G	V	G	A	P			–
K18R-hCT(18-32)	1956.7										**R**	F	H	T	F	P	Q	T	A	I	G	V	G	A	P			+
N17C-hCT(17-32)	2031.8									**C**	K	F	H	T	F	P	Q	T	A	I	G	V	G	A	P			–
N17F-hCT(17-32)	2075.9									**F**	K	F	H	T	F	P	Q	T	A	I	G	V	G	A	P			+
N17K-hCT(17-32)	2056.9									**K**	K	F	H	T	F	P	Q	T	A	I	G	V	G	A	P			–
A33 A34-hCT(18-34)	2070.9										K	F	H	T	F	P	Q	T	A	I	G	V	G	A	P	**A**	**A**	–
hCT(32-18)	1929.9										P	A	G	V	G	I	A	T	Q	P	F	T	H	F	K			–
Random sequence	2968.5	F	L	T	A	G	Q	N	T	I	Q	T	P	V	K	T	G	G	H	F	P	F	A	D	Y			–
Tat(47-57)	2031.9	G	Y	G	R	K	K	R	R	Q	R	R	R	G														+++
Penetratin(43-58)	2604.7	R	Q	I	K	I	W	F	Q	N	R	R	M	K	W	K	K												+++

[a] Calculated molecular weights of the peptides, including carboxyfluorescein.

[b] Significant internalization level is indicated by (+), whereas (–) indicates the absence of internalization over the mock experiment.

[c] Peptides numbering with respect to native human calcitonin. Amino acid modifications of the sequence highlighted in bold; k and f stand for D-lysine and D-phenylalanine, respectively. All fragments are labeled with carboxyfluorescein at the N-terminus; hCT-derived peptides and penetratin(43-58) and C-terminally amidated.

dium and mounted with or without fixation. Fixation was performed at room temperature for 30 min in 3% (v/v) formaldehyde before being rinsed with phosphate-buffered saline. The cells were then scanned using a Zeiss CLSM 410 inverted microscope (20) and 3D multichannel image processing was performed using the IMARIS software.

Endosome Staining

MDCK proliferating cells growing on four-well glass chamber slides were incubated with 4 mg/ml TRITC-dextran for 45 min to stain endosomes (26). Simultaneously, cells were incubated with 40 μM of hCT-derived peptide. Before CLSM observations, cells were fixed.

LIVE/DEAD Viability/Cytotoxicity Assay

MDCK cells were incubated at 4°C for 45 min with cold serum-free medium. Thereafter, serum-free medium was removed and replaced by serum-free medium (37°C) containing a mixture of 3 μM calcein AM (green stain of cytoplasm of enzymatically active viable cells, approx. 530 nm), and 6 μM ethidium homodimer (passage of damaged cells membranes and subsequent red stain of nuclei, > 600 nm) and MDCK were further incubated for 30 min at 37°C. Before CLSM observations, cells were washed three times with serum-free medium. To determine optimal dye concentration of ethidium homodimer, cells were killed using 70% methanol for 30 min.

LDH Release

The release of LDH indicates compromised cell membrane integrity. MDCK monolayers were grown on 12-well plates and incubated with carboxyfluorescein-labeled peptides at various concentrations and times of incubation. LDH release was estimated by withdrawing a 40-μl sample from each well and transferring it to 1 ml phosphate buffer (50 mM, pH 7.5) containing nicotinamide adenine dinucleotide (0.18 mM) and pyruvate (0.6 mM). The change in absorbance was measured at 340 nm using an UV spectrophotometer. Triton-X100 was used as positive control.

Investigation of hCT Receptor Expression on MDCK Cells by Measurement of cAMP Accumulation

MDCK cells were seeded onto 24-well plates at a density of 40,000 cells/well. Three days later the medium was replaced with a medium containing 136 mM NaCl, 5.4 mM KCl, 1 mM Na_2HPO_4, 5.5 mM glucose, 1 mM $CaCl_2$, 1 mM $MgCl_2$, 1 mM isobutylmethylxanthine, 0.1% bovine serum albumin, and 20 mM HEPES, pH 7.45. Incubation with test substances was performed at 37°C in a final volume of 200 μl for 15 min. Thereafter, the medium was replaced by 500 μl of ice-cold 95% ethanol containing 1 mM HCl, and cAMP was extracted at 4°C for 1 h. Ethanol was evaporated in a SpeedVac concentrator (Savant) and cAMP determined in reconstituted extracts by radioimmunoassay (RIA) as described by Moran *et al.* (27).

RESULTS

Cellular Uptake of hCT-Derived Peptides in MDCK Cell Monolayers and Tat(47-57) and Penetratin(43-58) in both MDCK and HeLa Cells

The distributions of carboxyfluorescein and carboxyfluorescein-labeled hCT-derived peptides were followed in living, nonfixed MDCK cell monolayers grown either on cell culture inserts (transepithelial electrical resistance = 111 ± 21 Ω·cm^2, n = 68) or glass chamber slides. The localization of Tat(47-57) and penetratin(43-58) within fixed or nonfixed MDCK cell monolayers and HeLa grown on glass chamber slides was also determined. No intracellular fluorescence was observed when the cells were incubated for 45 min with the negative controls, that is, no peptide (Fig. 1A), 40 μM nonconjugated carboxyfluorescein (Fig. 1B), or 40 μM random sequence (Fig. 1C). The latter, however, showed an extracellular fluorescence pattern. When incubated for 45 min at 37°C with MDCK cell monolayers the intracellular hCT-derived peptides (40 μM) demonstrated a punctuated cytoplasmic distribution (Figs. 1D and 1E). The translocation efficiency of peptides visually decreased in the order of hCT(9-32) ≈ hCT(12-32) > hCT(15-32) > hCT(18-32) (Table I). Although even the shortest fragment hCT(18-32) displayed some degree of translocation, the longest fragments such as hCT(9-32) and hCT(12-32) demonstrated visually a higher degree of uptake, as assessed by the apparent fluorescence intensity of the CLSM micrographs. All internalized fragments demonstrated a sectoral distribution, as intracellular fluorescence was observed only in some regions of the monolayers and not homogeneously distributed across the cell layers (Figs. 1F and 1G). Other than fluorescence no other visually detectable differences between the cell regions with and without translocation were observed. When assayed at 4°C the hCT-derived peptides were not translocated into the cells. The fully preserved viability of the cells at 4°C was assessed with the LIVE/DEAD Viability/Cytotoxicity Assay Kit (data not shown).

To elucidate the underlying principles of the cellular uptake, the amino acid sequence of hCT(18-32) was modified as follows (for details, see Table I). When lysine in position 18 was replaced by another basic residue, such as arginine, the capacity for translocation was conserved. Nevertheless, replacement by a non-charged amino acid, for example, alanine, or by a D-lysine abolished the uptake. Abolition of the uptake was also observed when exchanging the proline 23 with a more flexible residue, such as alanine. The extension of the sequence hCT(18-32) by coupling a phenylalanine to the N-terminus [N17F-hCT(17-32)], did not affect the capacity for translocation. On the other hand, when coupling a cysteine [N17C-hCT(17-32)] or a lysine [N17K-hCT(17-32)] to the N-terminus and two alanines to the C-terminus [A33A34-hCT(18-34)] translocation of the peptides was abolished. The importance of the orientation for peptide internalization was demonstrated since the reverse analog hCT(32-18) was not internalized. The role of the proline at the C-terminus seemed not to be crucial since hCT(18-31) could permeate the plasma membrane. However, the peptide hCT(9-29) was not internalized in MDCK cells, suggesting that the C-terminal domain is essential for cellular uptake.

The metabolic breakdown of hCT in contact with cells was previously found to initiate in the mid section of the peptide, that is, close to the N-terminus of hCT(18-32), predominantly through chymotryptic and tryptic-like cleavage (28). Therefore, it was believed that replacement of L- by D-amino acid residues in the hCT fragments would enhance their metabolic stability. The impact of such amino acid modifications upon membrane translocation was also investigated.

Exchange of L-phenylalanine in position 19 and L-lysine in position 18 by their D-enantiomers abolished the membrane translocating capacity of the peptides. Confocal microscopy pictures were identical to the negative controls as shown in Figs. 1A and 1B. The hCT(9-32) and hCT(12-32) fragments demonstrated similar punctuated cytoplasmic distributions whether the cells were grown on cell culture inserts or on glass chamber slides, providing evidence that the culture support had no influence on peptide uptake. Moreover, fixation of the cells before CLSM did not affect the pattern of internalization, except for a somewhat brighter fluorescence in fixed vs. nonfixed cells. Consequently, artifacts by fixation could be excluded. The fluorophore did not significantly alter peptide uptake, since hCT(9-32) fragments labeled either with carboxyfluorescein or TAMRA did not modify the cellular pattern with MDCK monolayers. These findings further support the results of Lang *et al.*, who demonstrated that the conjugation of fluorescein isothiocyanate (FITC) to hCT had no significant influence upon the transfer of peptides across excised nasal mucosa (29).

Concentration Effects of hCT-Derived Peptide upon Uptake into MDCK Cell Monolayers

To assess the effect of peptide concentration and to check for any saturation of the translocation, hCT(9-32), hCT(12-32) and hCT(18-32) were incubated with MDCK cells for 45 min at 10, 20, 40, and 100 μM. For CLSM inspection, cells remained nonfixed. Below the concentration of 40 μM only weak intracellular fluorescence was observed. At a concentration of 40 μM, detection was at optimum. At a peptide concentration of 100 μM, the intracellular fluorescence did not increase, instead accumulation of apical fluorescence, presumably fluorescent aggregates of the peptides, was detected on the cell layers (Fig. 1H). A similar aggregation pattern was also observed at 100 μM with hCT-derived peptides devoid of translocating abilities.

Effect of Incubation Time upon Uptake of hCT-Derived Peptides in MDCK Cell Monolayers

hCT(9-32), hCT(12-32), and hCT(18-32) were also incubated at 40 μM for four different times intervals: 15, 30, 45, and 60 min on MDCK cell monolayers. Negligible or poor internalization was observed at either 15 or 30 min. However, incubations for more than 30 min were sufficient for the vesicular internalization of peptides (data not shown).

Cellular Uptake of hCT-Derived Peptides in Proliferating MDCK Cells

The distribution of hCT(9-32), hCT(18-32), hCT (21–32), and random sequence (40 μM) was also investigated in proliferating MDCK cells after a 45-min incubation. For CLSM inspection cells were fixed. All fragments demonstrated a punctuated cytoplasmic distribution, clearly above the negative controls, that is, serum-free medium and fluorophore, respectively. The punctuated cytoplasmic distribution of hCT(18-32) is illustrated in Fig. 1 (data not shown for hCT(9-32), hCT(21-32), and random sequence). When hCT(9-32) was concomitantly incubated with TRITC-dextran (Fig. 1J), it was found to predominantly co-localize with TRITC-dextran (Fig. 1K), as indicated by the resulting yellow coloration (Fig. 1L), demonstrating the endocytotic nature of the cellular uptake of hCT-derived peptides. At the same time, the discrete observation of green and red vesicles indicated independent uptake of the peptide and the fluid phase endocytic marker (Fig. 1L). No uptake of TRITC-dextran was observed in confluent MDCK cells.

Cellular Uptake of Tat(47-57) and Penetratin(43-58) in MDCK Cell Monolayers and HeLa Cells

The highly positively charged carrier peptides Tat(47-57) and penetratin(43-58) were also incubated with MDCK monolayers for 1 h with a concentration of 10 μM. Tat(47-57) demonstrated a cytoplasmic and punctuated pattern in fixed cells. Although analogous to that observed with the hCT-derived peptides, the pattern was more uniformly distributed across the monolayers with Tat(47-57) (Figs. 2A and 2B). With penetratin(43-58), however, concomitant staining of the surface of the plasma membrane and intracellular translocation was observed (Figs. 2C and 2D). When using nonfixed MDCK cell monolayers, the intracellular patterns of the two cationic CPP were weaker but still punctuated and cytoplasmic. In living nonfixed and fixed HeLa cells, Tat(47-57) and penetratin(43-58) (10 μM) were mainly located in the cytoplasm with a punctuated distribution after 1 h of incubation (Figs. 2E and 2F).

Cytotoxicity of hCT(9-32), hCT(18-32), hCT(21-32), Tat(47-57), and Penetratin(43-58) on MDCK Cell Monolayers

hCT-derived peptides were incubated at 40 μM for three different incubation times: 30, 60, and 120 min (n = 4; Fig. 3A). Tat(47-57) and penetratin(43-58) peptides were incubated at a concentration of 10 μM during 60, 120, 180, and 240 min (n = 4; Fig. 3B). Triton X-100 (0.1% in serum-free medium) was used as positive control and serum-free medium as negative one. The results are represented as percentage of LDH release. The percentages were calculated by direct comparison to the positive control, that is, when the cell membranes were permeabilized by Triton X-100. The LDH release of the positive control was taken as 100%. As depicted in Figs. 3A and 3B, no significant differences in the percentage of LDH release were measured when the cells were incubated with serum-free medium alone or with peptide solutions. Therefore, none of the peptides tested in this study showed a relevant toxic effect on the MDCK cell monolayers, even after 4 h of incubation with Tat(47-57) and penetratin(43-58), at the indicated concentrations.

Assessment of hCT Receptor Expression on MDCK Cells

hCT, hCGRP, hADM, and hAmylin belong to a family of structurally and functionally related peptides that recognize their respective receptors with affinity in the nanomolar range (30), resulting in accumulation of cAMP. However, cross-reactivity of a given receptor with other peptides of the family is observed at high concentrations (micromolar range). We incubated MDCK cells with hCT, hCGRP, hADM, and hAmylin to verify whether the cells possess any calcitonin receptor activity and, if any, cross-reactivity was present. Forskolin, which stimulates adenylate cyclase, was used as a positive control to verify the capacity to produce cAMP. No sig-

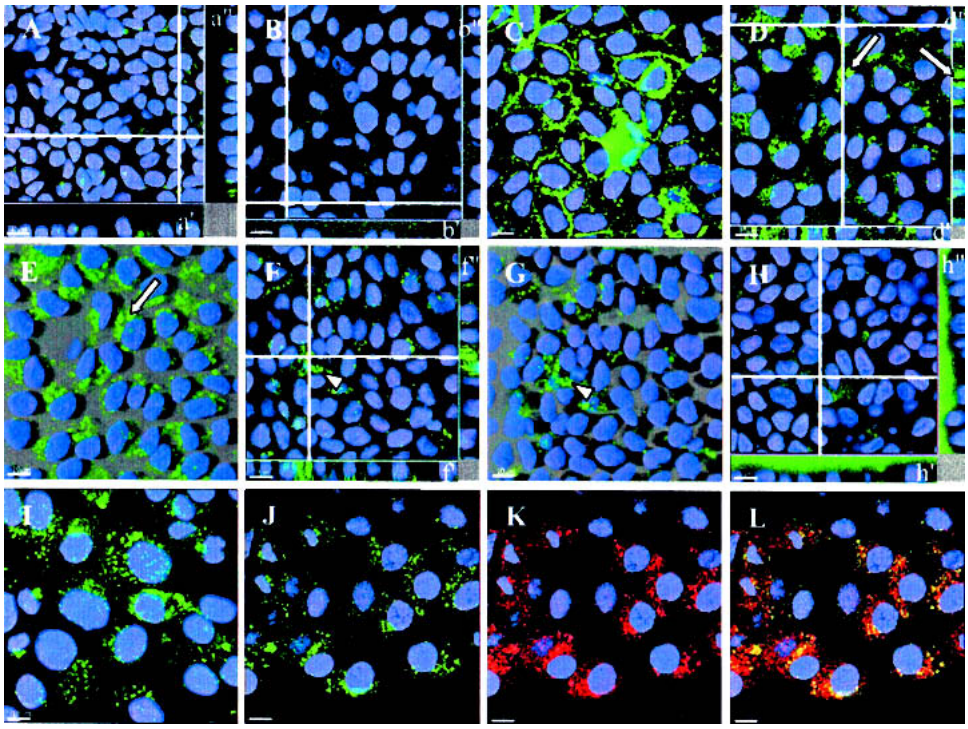

Fig. 1. (Legend on facing page.)

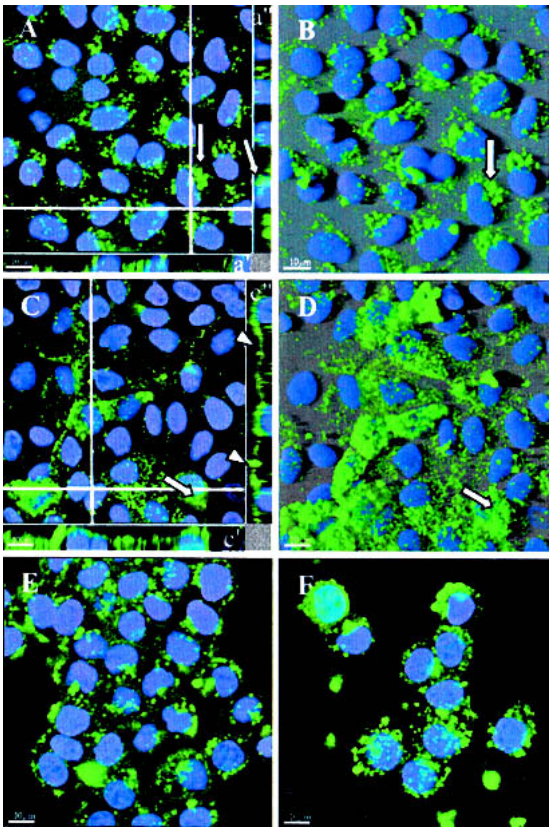

Fig. 2. (Legend on facing page.)

nificant accumulation of cAMP in response to hCT, hCGRP, hADM and hAmylin, was monitored (Fig. 4), cAMP levels remained in the range of untreated controls (2–7 pmol/well). MDCK appeared not to possess any calcitonin or calcitonin related receptor activity, thus suggesting that hCT-derived peptides use an alternative mechanism to translocate into MDCK.

DISCUSSION

Numerous peptide sequences derived from proteins with membrane translocating properties were previously investigated for their capacity as carrier peptides for the transfer of various cargoes into the cytosol of a variety of cells (4,5,31). Many of these CPP are highly positively charged and strongly interact with the negatively charged extracellular matrix of the plasma membrane (3,32). In the present study, we investigated the cell-penetrating capacities of peptides carrying relatively modest net positive charges or being neutral, namely C-terminal fragments of hCT, into a columnar-type epithelium, the MDCK monolayer using CLSM. hCT (9-32) was previously shown to translocate the plasma membrane of excised bovine nasal mucosa (22), and to act as a transfer vehicle for GFP into this tissue model (23). Prerequisite for assessing the capability of hCT-derived peptides to pass the plasma membrane of MDCK is direct detection and sufficient resolution by CLSM. However, several aspects need to be considered to interpret such observations. In principle, the observed intracellular fluorescence may be emitted by either intact peptides or metabolites still carrying the fluorophore.

For this study, we synthesized 20 different C-terminal sequences derived from hCT (see Table I). Seven of them translocated the plasma membrane of confluent MDCK monolayers. The shortest internalized hCT-derived peptide sequence was hCT(18-32). Shorter sequences lacked relevant translocating capacity, whereas longer fragments in fact permeated the cell membrane. The efficiency of translocation visually decreased in the order of hCT(9-32) ≈ hCT(12-32) > hCT(15-32) > hCT(18-32). We also looked at the important structural features required for internalization by modifications of the original amino acid sequence. Among these, we tried to increase the helicity of the peptide sequence in replacing the proline 23 by an alanine. This modification in fact abolished the internalization of the peptide and highlights the importance of the proline in this position. Among other reasons, the rigidity induced by the proline could be crucial for efficient peptide internalization. By replacing the lysine in position 18, we addressed the involvement of ionic interactions and the contribution of the positive charge on membrane translocation. The impact of a single positive net charge is expected to be much inferior to that of multiple positive charges as typically found in polycationic carrier peptides, for example, Tat(47-57). Polycationic CPPs have been previously reported to strongly interact with the extracellular matrix of plasma membranes (6,33). Nevertheless, there could be a contribution of the positive charge of the lysine in position 18 in anchoring the sequences at the bilayer surface. Replacement of lysine by noncharged alanine prevented peptide internalization, whereas maintaining the positive charge by replacing the lysine with an arginine maintained peptide internalization. However, the conformation of the positive charge at this position seemed to play a crucial role, since the replacement of *L*-lysine by *D*-lysine strikingly abolished uptake. Another role of the lysine in position 18 might be the inhibition of premature aggregation through charge repulsion. If not stabilized by a minimum positive charge hydrophobic interactions of the C-terminal domain could prevail and lead to premature aggregation, that is, inactivation of shorter hCT fragments than hCT(18-32). Nevertheless, this would not explain the failure of *D*-lysine replacement.

Sequence extension of hCT(18-32) beyond the N- and C-termini showed in most of the cases a loss of internalization except when phenylalanine was added to the N-terminus. Therefore, introduction of a peptidic spacer to serve as a cargo-linker, should be engineered at the N-terminus, possibly by adding a phenylalanine.

In most of the previous studies, cells incubated with polycationic CPP, demonstrated rapid peptide uptake with predominant nuclear localization and lack of punctuated cytoplasmic labeling, which is characteristic of endocytic uptake. Additionally, internalization of CPP was not significantly inhibited at low temperature, and structure-activity studies often suggested that internalization did not depend on the secondary structure, ruling out putative receptor recognition. It

Fig. 1. Confocal microscopy pictures of hCT derived peptides distribution in confluent MDCK monolayers and proliferating MDCK. MDCK cells forming monolayers were incubated for 45 min at 37°C without peptide (A), with 40 μM of carboxyfluorescein (B), with 40 μM of the random sequence (C), or with 40 μM of carboxyfluorescein-labeled hCT(12-32) (D–G). D and E show the punctuated cytoplasmic distribution of hCT(12-32). Intracellular vesicles are shown by arrows. E is the 3D projection of D. F and G illustrate the sectoral distribution of the peptide. The arrowheads point to areas where the peptide is internalized. G is the 3D projection of F. H shows MDCK cells forming monolayers incubated with 100 μM of carboxyfluorescein-labeled hCT(9-32). MDCK-proliferating cells were incubated for 45 min at 37°C with 40 μM of hCT(18-32) (I) and co-incubated with 40 μM of hCT(9-32) together with 4 mg/ml of TRITC-dextran for endosomal staining (J–L). J: hCT(9-32) (green fluorescence); K: TRITC-dextran (red fluorescence); L: co-localization (yellow fluorescence) of hCT(9-32) peptide and TRITC-dextran. The cell nuclei are shown in blue, the peptide and carboxyfluorescein in green. Processed data sets are illustrated as xy-sections for A–D, F, H–L. a′, b′, d′, f′, and h′ are xz projections, and a′′, b′′, d′′, f′′, and h′′ are yz projections. The white lines indicate the position of the sections. Bars: 10 μm. Interpretation of C needs to be restricted to areas where the optical section is on the level of the nuclei.

Fig. 2. Cellular uptake of Tat(47-57) and penetratin(43-58) in MDCK and HeLa cells. MDCK cells forming monolayers were incubated for 1 h with 10 μM carboxyfluorescein-labeled Tat(47-57) (A, B) and penetratin(43-58) (C, D). HeLa cells were incubated for 1 h with 10 μM carboxyfluorescein-labeled Tat(47-57) and penetratin(43-58), respectively (E and F). Arrows in A and B point to the punctuated cytoplasmic distribution of Tat(47-57). Arrows in C and D show the punctuated cytoplasmic distribution of Penetratin(43-58) and arrowheads the fluorescent peptide located on the surface of the plasma membrane. Micrographs A, C, E, and F are section micrographs (A, C, E, F: xy section; a′, c′: xz projection; a′′, c′′: yz projection), whereas B and D are the respective 3D projections. The cell nuclei are shown in blue, the peptide in green. The white lines indicate the position of the sections. Bars: 10 μm.

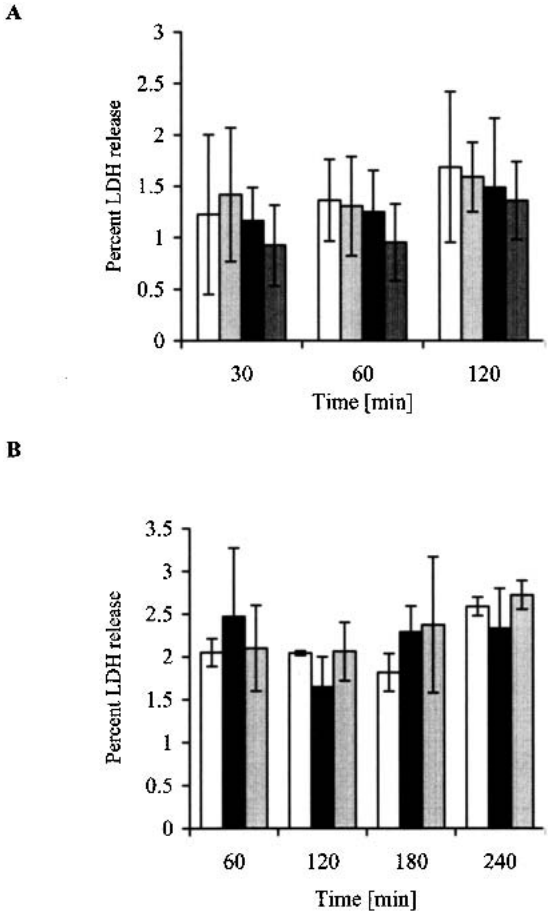

Fig. 3. Determination of LDH release. MDCK cell monolayers were incubated 30, 60, 120, 180, and 240 min with serum-free medium for control (white). A, MDCK cells were incubated 30, 60, and 120 min with 40 μM hCT(9-32) (light gray), hCT(18-32) (black), and hCT(21-32) (dark gray). B, MDCK cells were incubated 60, 120, 180, and 240 min with 10 μM Tat(47-57) (black) and penetratin(43-58) (light gray). The release of LDH is depicted relative to the release amount of LDH from epithelium exposed to 0.1% Triton X-100. No relevant toxicity is observed. Mean ± SD (n = 4).

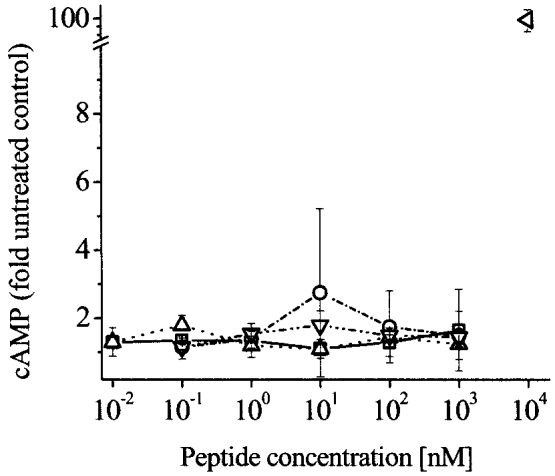

Fig. 4. Investigation of hCT receptor on MDCK plasma membrane. MDCK cells forming monolayers were incubated with different concentrations of hCT (□), hAmylin (◯), hCGRP (△), and hADM (▽). Accumulation of cAMP was measured to investigate the presence of hCT- or hCT-related peptides receptors on plasma membrane of MDCK cells. The level of cAMP accumulation remained in the range of nontreated cells. Therefore, no hCT, hAmylin, hCGRP, and hADM receptors are expressed on MDCK plasma membrane. Forskolin (◁) was used as a control to verify the cells capacity to produce cAMP. All experiments were repeated two times (n = 2). The results were expressed as the ratio of stimulated and untreated controls. Mean ± SD.

was thus commonly accepted that the internalization of CPPs would not involve endocytosis or specific protein transporters. Instead, passive transfer through the lipid bilayer has been proposed as a possible mechanism of translocation (3,6,9,10,16). Recent studies, however, contrast with this hypothesis, after a punctuated cytoplasmic distribution of Tat(48-60) and poly-arginine in HeLa and CHO cells was observed (18). Koppelhus *et al.* showed that a PNA conjugated to C-Tat(48-60) or a modified penetratin(42-58) was found to predominantly segregate in endocytic vesicles (17). Both of them described an energy-dependent uptake mechanism.

In the present study, we demonstrated a sectoral, punctuated cytoplasmic localization of translocated hCT-derived peptides and the absence of any nuclear fluorescence. This latter fact may be explained by the absence of a nuclear translocating motif in the sequence of the investigated peptides. Yet, without further knowledge, explanation for the observed sectoral distribution is still elusive. In addition, our study suggested an energy-, time- and concentration-dependent mechanism. However, at concentrations above 100 μM the hydrophobic C-termini of the hCT-derived peptides appear to strongly interact and lead to the formation of aggregates as thoroughly studied for hCT itself (34). Premature aggregation of a peptide would efficiently prevent its internalization in a non-concentration-dependent manner. The absence of significant translocation of distinct modifications, particularly of hCT(32-18), *D*-K18-hCT(18-32) and *D*-F19-hCT(18-32), vs. translocation of others, does not exclude the involvement of a receptor-dependent mechanism. However, owing to the demonstrated absence of hCT and hCT-related receptors on MDCK plasma membranes, the involvement of this receptor must be excluded. Nevertheless, an alternative receptor to the calcitonin receptor might assist in peptide internalization.

For comparison, Tat(47-57) showed a punctuated cytoplasmic pattern, indicating endocytic vesicles, whereas penetratin(43-58) depicted both a cytoplasmic and punctuated pattern, and an extracellular staining of the cell membrane. However, when incubated with HeLa cells, both Tat(47-57) and penetratin(43-58) demonstrated a similar punctuated cytoplasmic pattern. In MDCK and HeLa cells both peptides demonstrated only weak nuclear uptake. Contrasting to the present results, two independent studies recently claimed that Tat(48-57) and Tat(44-57) cannot permeate MDCK plasma membrane (35,36). Nevertheless, distinct differences in both the Tat sequences, the cell culture and other experimental protocols limit the possibilities to interpret this discrepancy here.

Our data strongly support the involvement of endocytosis as the major route for the internalization of hCT-derived peptides, Tat(47-57) and penetratin(43-58) into MDCK monolayers, in contrast to the direct cytosolic pathway suggested for other peptides (3,6,10). However, it is important to note

that the efficiency of peptide uptake was dependent upon both cell line and peptide sequence. HeLa cells demonstrated a greater uptake potential than MDCK cells, and Tat(47-57) was more readily internalized as compared to the hCT-derived peptides. These results indicate that the uptake probably depends on a cell-specific membrane component or the specific lipid composition of the membrane. The endocytic pathway can expose peptide, protein and nucleic acid based-therapeutics to late endosomal and lysosomal degradation and, therefore, may represent a problematic pathway for drug delivery. A recent study showed that when fused to Tat(47-57), lysosomal β-glucuronidase was internalized by endocytosis and the fusion protein's enzyme activity restored in a mouse model of β-glucuronidase deficiency (37). This demonstrates that a translocated cargo may retain its biological activity even when transported via an endocytic pathway. Alternatively, endosomal/lysosomal degradation could be considered as an attractive feature to release the therapeutic principle from its conjugate. This would necessitate the existence of a suitable metabolically cleavable spacer between cargo and peptide.

Recently, artifactual uptake of some CPPs was demonstrated upon strong and even mild fixation conditions (18,38). In our study, under both fixed and nonfixed conditions, HeLa cells showed a similar fluorescence pattern, indicating the absence of experimental artifacts upon fixation. Supporting this view is the recent study of Koppelhus *et al*. demonstrating that fixation did not negatively effect the vesicular translocation pattern of PNA conjugated to CPPs (17). Nevertheless, nonfixed MDCK cells demonstrated a somewhat weaker but otherwise identical, punctuated cytoplasmic fluorescence (not shown). This result is explained by a higher bleaching of carboxyfluorescein in nonfixed cells vs. fixed cells (39). In case of artifactual redistribution of the peptides after fixation, a predominantly nuclear localization and the lack of punctuated cytoplasmic labeling characteristics of endocytic uptake would be expected, as reported in most published data on fixed cells (3,10,16).

Interestingly, we found an nonspecific uptake of all the tested hCT-derived sequences by proliferating MDCK cells, whereas selected peptides only were internalized by confluent MDCK. PNA-peptide conjugates also demonstrate faster cellular uptake when using less confluent cells, demonstrating an influence of the physiologic state of the cells relative to peptide uptake (17). Our findings may point to a more complex and less general mechanism for the uptake of hCT-derived peptides in MDCK monolayers as compared to proliferating cells.

The release of cytoplasmic LDH into the cell culture supernatant was studied to assess plasma membrane damage when MDCK cell monolayers were incubated with hCT-derived peptides, Tat(47-57) and penetratin(43-58). No significant toxicity induced by the tested peptides was detected. Koppelhus *et al*. described a diffuse, strong staining of both the cytoplasm and the nuclei when the peptides were toxic (17). The well-defined, punctuated cytoplasmic pattern, described in the present work, provides further support in demonstrating that the peptide sequences used in this study did no exert significant toxicity when incubated with either MDCK or HeLa.

In conclusion, we propose a new family of modestly cationic peptides, all derived from human calcitonin, that are able to translocate MDCK plasma membrane. The translocated hCT peptides demonstrated a sectoral and punctuated cytoplasmic distribution. Polycationic CPP such as Tat(47-57) and penetratin(43-58) also showed a punctuated cytoplasmic distribution in MDCK and HeLa cells. The results obtained in our study in combination with those of other laboratories lend support to endocytosis as the common mechanism for peptide translocation. At this point, it is difficult to outline the structural requirements for efficient internalization of hCT-derived peptides. Moreover, the observed structure-activity relationship of studied peptides may also relate to variations in their aggregation potential, as well as differences in their pathway and rate of metabolism. Work is undergoing to assess the different metabolism kinetics of selected hCT-derived peptides and to optimize the translocating abilities of hCT-derived peptides. Therefore, further studies need to be performed to identify an optimized sequence for translocation and mechanism of action of our CPP.

ACKNOWLEDGMENTS

The authors acknowledge the following contributions: Professor Heidi Wunderli-Allenspach, Maja Günthert (ETH Zurich), and Barbara Rothen-Rutishauser (University of Bern) for their introduction to the confocal microscopy techniques; Professor Kurt Ballmer (Paul Scherrer Institut, Villigen) for his advice on the uptake experiments; and Dr. Stefan R. K. Hoffmann (University of Zurich) for the purification of Tat and penetratin. This work was supported by ETH Zurich, research project number 0-20702-99 and the Commission of the European Union (EU project on Quality of Life and Management of Living Resources, Project No. QLK2-CT-2001-01451).

REFERENCES

1. A. M. Gewirtz, D. L. Sokol, and M. Z. Ratajczak. Nucleic acid therapeutics: state of the art and future prospects. *Blood* **92**:712–736 (1998).
2. R. L. Juliano, S. Alahari, H. Yoo, R. Kole, and M. Cho. Antisense pharmacodynamics: critical issues in the transport and delivery of antisense oligonucleotides. *Pharm. Res.* **16**:494–502 (1999).
3. E. Vives, P. Brodin, and B. Lebleu. A truncated HIV-1 Tat protein basic domain rapidly translocates through the plasma membrane and accumulates in the cell nucleus. *J. Biol. Chem.* **272**: 16010–16017 (1997).
4. S. R. Schwarze, A. Ho, A. Vocero-Akbani, and S. F. Dowdy. In vivo protein transduction: delivery of a biologically active protein into the mouse. *Science* **285**:1569–1572 (1999).
5. V. Polyakov, V. Sharma, J. L. Dahlheimer, C. M. Pica, G. D. Luker, and D. Piwnica-Worms. Novel Tat-peptide chelates for direct transduction of technetium-99m and rhenium into human cells for imaging and radiotherapy. *Bioconjug. Chem.* **11**:762–771 (2000).
6. D. Derossi, S. Calvet, A. Trembleau, A. Brunissen, G. Chassaing, and A. Prochiantz. Cell internalization of the third helix of the antennapedia homeodomain is receptor-independent. *J. Biol. Chem.* **271**:18188–18193 (1996).
7. G. Elliott and P. O'Hare. Intercellular trafficking of VP22-GFP fusion proteins. *Gene Ther.* **6**:149–151 (1999).
8. N. Brewis, A. Phelan, J. Webb, J. Drew, G. Elliott, and P. O'Hare. Evaluation of VP22 spread in tissue culture. *J. Virol.* **74**: 1051–1056 (2000).
9. P. A. Wender, D. J. Mitchell, K. Pattabiraman, E. T. Pelkey, L. Steinman, and J. B. Rothbard. The design, synthesis, and evaluation of molecules that enable or enhance cellular uptake: pep-

toid molecular transporters. *Proc. Natl. Acad. Sci. USA* **97**:13003–13008 (2000).
10. S. Futaki, T. Suzuki, W. Ohashi, T. Yagami, S. Tanaka, K. Ueda, and Y. Sugiura. Arginine-rich peptides. An abundant source of membrane-permeable peptides having potential as carriers for intracellular protein delivery. *J. Biol. Chem.* **276**:5836–5840 (2001).
11. M. Pooga, U. Soomets, M. Hallbrink, A. Valkna, K. Saar, K. Rezaei, U. Kahl, J. X. Hao, X. J. Xu, Z. Wiesenfeld-Hallin, T. Hokfelt, T. Bartfai, and U. Langel. Cell penetrating PNA constructs regulate galanin receptor levels and modify pain transmission in vivo. *Nat. Biotechnol.* **16**:857–861 (1998).
12. A. Astriab-Fisher, D. Sergueev, M. Fisher, B. R. Shaw, and R. L. Juliano. Conjugates of antisense oligonucleotides with the Tat and antennapedia cell-penetrating peptides: effects on cellular uptake, binding to target sequences, and biologic actions. *Pharm. Res.* **19**:744–754 (2002).
13. H. Nagahara, A. M. Vocero-Akbani, E. L. Snyder, A. Ho, D. G. Latham, N. A. Lissy, M. Becker-Hapak, S. A. Ezhevsky, and S. F. Dowdy. Transduction of full-length TAT fusion proteins into mammalian cells: TAT-p27Kip1 induces cell migration. *Nat. Med.* **4**:1449–1452 (1998).
14. M. Lewin, N. Carlesso, C. H. Tung, X. W. Tang, D. Cory, D. T. Scadden, and R. Weissleder. Tat peptide-derivatized magnetic nanoparticles allow in vivo tracking and recovery of progenitor cells. *Nat. Biotechnol.* **18**:410–414 (2000).
15. V. P. Torchilin, R. Rammohan, V. Weissig, and T. S. Levchenko. TAT peptide on the surface of liposomes affords their efficient intracellular delivery even at low temperature and in the presence of metabolic inhibitors. *Proc. Natl. Acad. Sci. USA* **98**:8786–8791 (2001).
16. T. Suzuki, S. Futaki, M. Niwa, S. Tanaka, K. Ueda, and Y. Sugiura. Possible existence of common internalization mechanisms among arginine- rich peptides. *J. Biol. Chem.* **277**:2437–2443 (2002).
17. U. Koppelhus, S. K. Awasthi, V. Zachar, H. U. Holst, P. Ebbesen, and P. E. Nielsen. Cell-dependent differential cellular uptake of PNA, peptides, and PNA- peptide conjugates. *Antisense Nucleic Acid Drug Dev.* **12**:51–63 (2002).
18. J. P. Richard, K. Melikov, E. Vives, C. Ramos, B. Verbeure, M. J. Gait, L. V. Chernomordik, and B. Lebleu. Cell-penetrating peptides: A re-evaluation of the mechanism of cellular uptake. *J. Biol. Chem.* **30**:585–590 (2003).
19. C. R. Gaush, W. L. Hard, and T. F. Smith. Characterization of an established line of canine kidney cells (MDCK). *Proc. Soc. Exp. Biol. Med.* **122**:931–935 (1966).
20. B. Rothen-Rutishauser, S. D. Kramer, A. Braun, M. Gunthert, and H. Wunderli-Allenspach. MDCK cell cultures as an epithelial in vitro model: cytoskeleton and tight junctions as indicators for the definition of age-related stages by confocal microscopy. *Pharm. Res.* **15**:964–971 (1998).
21. M. Lindgren, M. Hallbrink, A. Prochiantz, and U. Langel. Cell-penetrating peptides. *Trends Pharmacol. Sci.* **21**:99–103 (2000).
22. M. C. Schmidt, B. Rothen-Rutishauser, B. Rist, A. Beck-Sickinger, H. Wunderli-Allenspach, W. Rubas, W. Sadee, and H. P. Merkle. Translocation of human calcitonin in respiratory nasal epithelium is associated with self-assembly in lipid membrane. *Biochemistry* **37**:16582–16590 (1998).
23. Z. Machova, C. Muhle, U. Krauss, R. Trehin, A. Koch, H. P. Merkle, and A. G. Beck-Sickinger. Cellular internalization of enhanced green fluorescent protein ligated to a human calcitonin-based carrier peptide. *Chembiochem.* **3**:672–677 (2002).
24. B. Rist, M. Entzeroth, and A. G. Beck-Sickinger. From micromolar to nanomolar affinity: A systematic approach to identify the binding site of CGRP at the human calcitonin gene-related peptide 1 receptor. *J. Med. Chem.* **41**:117–123 (1998).
25. P. J. A. Weber, J. E. Bader, G. Folkers, and A. G. Beck-Sickinger. A fast and inexpensive method for N-terminal fluorescein-labeling of peptides. *Bioorg. Med. Chem. Lett.* **8**:597–600 (1998).
26. N. Courret, C. Frehel, N. Gouhier, M. Pouchelet, E. Prina, P. Roux, and J. C. Antoine. Biogenesis of Leishmania-harbouring parasitophorous vacuoles following phagocytosis of the metacyclic promastigote or amastigote stages of the parasites. *J. Cell Sci.* **115**:2303–2316 (2002).
27. J. Moran, W. Hunziker, and J. A. Fischer. Calcitonin and calcium ionophores: cyclic AMP responses in cells of a human lymphoid line. *Proc. Natl. Acad. Sci. USA* **75**:3984–3988 (1978).
28. S. R. Lang, W. Staudenmann, P. James, H. J. Manz, R. Kessler, B. Galli, H. P. Moser, A. Rummelt, and H. P. Merkle. Proteolysis of human calcitonin in excised bovine nasal mucosa: Elucidation of the metabolic pathway by liquid secondary ionization mass spectrometry (LSIMS) and matrix assisted laser desorption ionization mass spectrometry (MALDI). *Pharm. Res.* **13**:1679–1685 (1996).
29. S. Lang, B. Rothen-Rutishauser, J. C. Perriard, M. C. Schmidt, and H. P. Merkle. Permeation and pathways of human calcitonin (hCT) across excised bovine nasal mucosa. *Peptides* **19**:599–607 (1997).
30. R. Muff, W. Born, and J. A. Fischer. Calcitonin, calcitonin gene-related peptide, adrenomedullin and amylin: homologous peptides, separate receptors and overlapping biological actions. *Eur. J. Endocrinol.* **133**:17–20 (1995).
31. A. Eguchi, T. Akuta, H. Okuyama, T. Senda, H. Yokoi, H. Inokuchi, S. Fujita, T. Hayakawa, K. Takeda, M. Hasegawa, and M. Nakanishi. Protein transduction domain of HIV-1 Tat protein promotes efficient delivery of DNA into mammalian cells. *J. Biol. Chem.* **276**:26204–26210 (2001).
32. M. Lindgren, X. Gallet, U. Soomets, M. Hallbrink, E. Brakenhielm, M. Pooga, R. Brasseur, and U. Langel. Translocation properties of novel cell penetrating transportan and penetratin analogues. *Bioconjug. Chem.* **11**:619–626 (2000).
33. L. A. Kueltzo and C. R. Middaugh. Potential use of non-classical pathways for the transport of macromolecular drugs. *Expert Opin. Invest. Drugs.* **9**:2039–2050 (2000).
34. H. H. Bauer, U. Aebi, M. Haner, R. Hermann, M. Muller, and H. P. Merkle. Architecture and polymorphism of fibrillar supramolecular assemblies produced by in vitro aggregation of human calcitonin. *J. Struct. Biol.* **115**:1–15 (1995).
35. S. Violini, V. Sharma, J. L. Prior, M. Dyszlewski, and D. Piwnica-Worms. Evidence for a plasma membrane-mediated permeability barrier to tat basic domain in well-differentiated epithelial cells: lack of correlation with heparan sulfate. *Biochemistry* **41**:12652–12661 (2002).
36. S. D. Krämer and H. Wunderli-Allenspach. No entry for TAT(44-57) into liposomes and intact MDCK cells: novel approach to study membrane permeation of cell-penetrating peptides. *Biochim. Biophys. Acta* **1609**:161–169 (2003).
37. H. Xia, Q. Mao, and B. L. Davidson. The HIV Tat protein transduction domain improves the biodistribution of beta-glucuronidase expressed from recombinant viral vectors. *Nat. Biotechnol.* **19**:640–644 (2001).
38. M. Lundberg and M. Johansson. Positively charged DNA-binding proteins cause apparent cell membrane translocation. *Biochem. Biophys. Res. Commun.* **291**:367–371 (2002).
39. C. Pichon, M. Monsigny, and A. C. Roche. Intracellular localization of oligonucleotides: influence of fixative protocols. *Antisense Nucleic Acid Drug Dev.* **9**:89–93 (1999).